JBUON 2018; 23(3): 800-813
ISSN: 1107-0625, online ISSN: 2241-6293 • www.jbuon.com
E-mail: editorial_office@jbuon.com

ORIGINAL ARTICLE

Chitosan-capped gold nanoparticles impair radioresistant glioblastoma stem-like cells

Mihaela Aldea[1], Monica Potara[2], Olga Soritau[3], Ioan Stefan Florian[4], Adrian Florea[5], Timea Nagy-Simon[2], Valentina Pileczki[6], Ioana Brie[1,3], Dana Maniu[7], Gabriel Kacso[1,8]

[1]Department of Medical Oncology and Radiotherapy, Iuliu Hatieganu University of Medicine and Pharmacy, Cluj-Napoca, Romania; [2]Nanobiophotonics and Laser Microscopy Center, Interdisciplinary Research in Bio-Nano-Sciences, and Faculty of Physics, Babes-Bolyai University, Cluj-Napoca, Romania; [3]Department of Tumor Biology, Ion Chiricuta Cancer Institute, Cluj-Napoca, Romania; [4]Department of Neurosurgery, Iuliu Hatieganu University of Medicine and Pharmacy, Cluj-Napoca, Romania; [5]Department of Cell and Molecular Biology, Iuliu Hatieganu University of Medicine and Pharmacy, Cluj-Napoca, Romania; [6]The Research Center for Functional Genomics, Biomedicine and Translational Medicine, "Iuliu Hatieganu" University of Medicine and Pharmacy, Cluj-Napoca, Romania; [7]Department of Biomolecular Physics, Faculty of Physics, Babes-Bolyai University, Cluj-Napoca, Romania [8]Amethyst Radiotherapy Center, Cluj, Romania

Summary

Purpose: *Glioblastoma is a rapidly evolving lethal disease mainly due to its highly chemo- and radioresistant glioblastoma stem cells (GSCs). Herein, we tested if chitosan-capped gold nanoparticles (Chit-GNPs) may overcome the limitations of drug concentrations by increased cell internalization in GSCs and if such GNPs could enhance the response to irradiation.*

Methods: *Chitosan was used for Chit-GNP synthesis as a reducing and stabilizing agent. Chit-GNPs were characterized by spectroscopy, dark field, transmission electron microscopy and zeta potential measurements. Patient-derived GSCs and human osteoblasts were treated with increasing concentrations of nanoparticles and irradiated. The uptake and cytotoxicity of Chit-GNPs were compared to that of uncoated GNPs.*

Results: *The positively-charged, 26 nm-sized, spherical Chit-GNPs, showed a huge intracellular accumulation into the cytosol, lysosomes and near the nucleus, whereas no uncoated GNPs were internalized within GSCs. Surprisingly, Chit-GNPs were highly cytotoxic for GSCs irrespective of cell irradiation, that failed to add an additional benefit when combined with Chit-GNPs/GNPs. Moreover, Chit-GNPs were selectively cytotoxic for GSCs and did not affect the normal cells, despite an increased nanoparticle internalization.*

Conclusions: *The important Chit-GNP internalization and their selective cytotoxicity for GSCs make this compound a potential novel anticancer agent and a promising backbone for drug delivery in glioblastoma.*

Key words: *cancer stem cells, chitosan, glioblastoma, gold nanoparticles, radiotherapy*

Introduction

Glioblastoma is a rapidly lethal primary brain cancer with a stringent need for new treatment strategies [1]. Conventional treatments offer only a modest survival benefit, mainly because of the highly chemo- and radioresistant GSCs, that will eventually lead to disease recurrence and inevitable death [2-6].

Increased DNA repair capacity and enhanced expression of ATP-binding cassette drug transporters shield GSCs from conventional treatments and explain their aggressive behavior [7]. This daunting treatment resistance may be overcome by the use of nanotechnology, which provides appealing strategies for preferential drug accumulation,

Correspondence to: Mihaela Aldea, MD. Republicii str, no 34-36, 400012, Cluj-Napoca, Romania.
Tel: +40 741007967, E-mail: mihaela.aldea1@gmail.com
Received: 16/10/2017; Accepted: 09/11/2017

controlled-release of anticancer agents or specific targeting of cancer cells, with the aim of attaining effective drug concentrations in the tumor and minimal toxicity on healthy tissues [8,9].

Moreover, nanotechnology may open new avenues in addressing radioresistance. One interesting method would be the use of heavy metal nanoparticles (NPs) as radio-expanders in order to enhance the radiation from the "inside" of the tumor when a relatively low radiation source is applied from the "outside". This phenomenon is termed the "Compton effect" and implies that irradiated high Z nanoparticles (such as gold nanoparticles = GNP) would be able to boost local radiation levels by secondary radiation produced by nanoparticles, through photoelectric effect (mainly) and/or Compton effect. The limitation of the impact in the immediate vicinity of GNP conglomerates has the advantage of sparing unnecessary brain damage [8,10,11].

In this study, we synthetized Chit-GNPs in order to overcome the limitations of drug concentrations by an increased cell internalization within GSCs and we tested if such gold NPs could enhance the radiation response of GSCs with high (MV) and low (kV) energy sources of irradiation.

Methods

Materials

Chitosan (medium molecular weight), hydrogen tetrachloroaurate(III) trihydrate ($HAuCl_4 \cdot 3H_2O$) and trisodium citrate ($C6H5Na3O7 \cdot 2H_2O$) were purchased from Sigma-Aldrich, St.Louis, USA. Glacial acetic acid and sodium were obtained from Merck, Darmstadt, Germany. Glacial acetic acid was diluted to a 1% aqueous solution before use. Chitosan was dissolved in 1% acetic acid solution. Ultrapure water was used in all aqueous solutions and rinsing procedures.

Nanoparticles synthesis

GNPs were prepared following the Turkevich–Frens method [12]. Briefly, 100 mL of $HAuCl_4 \cdot 3H_2O$ (10^{-3} M) were brought to boil and a solution of trisodium citrate (10 mL, 38.8×10^{-3} M) was added at once under vigorous stirring. Stirring and boiling have been continued for another 10–15 min after the color of the colloid became deep-red burgundy. The solution was then removed from heat and the stirring process was continued for another 15 min. Chit-GNPs were obtained according to a slightly modified version of the method described in our previous work [13]. In a typical procedure, 3 ml of 10^{-3} M $HAuCl_4$ were added to 18 ml of 2 mg/mL chitosan solution, and then the mixture was heated to 50°C and kept at this temperature under magnetic stirring. The synthesis process was completed within a total 2 hrs under magnetic stirring. The colloidal solutions were purified by centrifugation and re-suspended in ultrapure water.

Structural characterization of NPs

Optical extinction spectra of NPs were collected in a 2 mm quartz cell using a Jasco V-670 spectrophotometer with 1 nm spectral resolution. The zeta potential of colloidal particles dispersed in ultrapure water was recorded at 25 °C using a Malvern Zetasizer Nano ZS-90 instrument. The concentration of gold in the colloidal suspension (μg/mL) was determined by atomic absorption spectroscopy (Avanta PM, GBC-Australia).

Transmission electron microscopy (TEM) was used to determine the median size of NPs. Five μl GNPs in suspension were added on 300 mesh copper grids (Agar Scientific Ltd., Stansted, UK) previously covered with a thin layer of formvar (Electron Microscopy Sciences, Hatfield, USA). After 5 min, the excess of liquid was removed with filter paper and the GNPs were examined with a JEOL JEM 1010 transmission electron microscope (JEOL Ltd., Japan) operating at 80 kV acceleration voltage. Images were captured using a Mega VIEW III camera (Olympus, Soft Imaging System, Germany). The diameters of GNPs (n= 600 for either type of particles) were manually measured on the TEM photographs using CellD morphometry software (Olympus Soft Imaging Solutions GMBH, Munster, Germany). The mean diameters and standard deviations were calculated, and the size distribution was graphically represented using Microsoft Excel (Microsoft Corporation, Redmond, USA).

Cell cultures

GM1, Gbl8 and Gbl12 primary glioblastoma cell lines were isolated from freshly resected glioblastoma specimens as previously described by our team [14]. Cells were cultured in a serum-free medium containing epidermal growth factor (EGF), basic fibroblast growth factor (FGF), and B27 supplement. GM1 cells express the stem cell markers CD133, CD105, CD90, Nanog, Oct 3/4, CXCR4, nestin, and neural markers, such as glial fibrillary acidic protein (GFAP), neurofilament protein (NF) and human glyceraldehyde 3-phosphate dehydrogenase (GAPDH). Cells also display a high proliferative potential despite chemotherapy and irradiation and also have the ability to form spheroids in suspension [14].

After isolation in serum-free medium and expansion, cells were cultured in Ham's F-12 and DMEM media used in 1:1 ratio, supplemented with 15% fetal calf serum (FCS), 100 U/ml penicillin and 100 μg/ ml streptomycin, 2mM L-glutamine, 1% non-essential amino acids (NEA), 55 μM beta-mercaptoethanol and 1 mM sodium pyruvate.

Primary human osteoblasts (OBL) served as "normal cell model" and were cultured in complex osteogenic medium consisting of DMEM/F-12 medium with 10% FCS, 2mM L-glutamine, 1% NEA, antibiotics, 10 nM dexamethasone, 50 μg/ml ascorbic acid and 10 mM β-glycero-phosphate.

Cultures were maintained at 37°C in a humidified atmosphere of 95 % air and 5% CO_2. Where not otherwise specified, all cell culture reagents were purchased from Sigma-Aldrich Corporation (St Louis, MO, USA).

Gbl 8, Gbl 12 characterization through immunocytochemistry

For phenotypic characterization immunocytochemical staining was performed. The isolated glioblastoma cells were cultured on 8-wells Nunc™ Lab-Tek™ chamber-slides in complete standard stem cell medium. After 3 days cell monolayers were fixed with 4% paraformaldehyde solution in PBS followed by a permeabilization step with 0.1% Triton X-100 in PBS for 20 min at room temperature. Unspecific antibody binding was blocked with 10% BSA (bovine serum albumin) in PBS, 20 min at room temperature. Incubation with the primary antibodies was performed at 4°C during the night. Primary monoclonal antibodies used were: CD 133, Nestin, Sox-2 (Santa Cruz Biotechnology, dilution 1:50 in 1% BSA in PBS), Nanog (R&D dilution 1:100), GFAP and neurofilaments (NF) (Sigma dilution 1:100), all mouse anti-human antibodies. Secondary goat anti-mouse antibodies IgG marked with FITC and IgM Phycoerythrin (Santa Cruz Biotechnologies) were used respecting the same dilution, with incubation 45–60 min at 37°C. Each staining step was followed by three washes with PBS. For highlighting of nuclei, antifade medium containing DAPI (4,6-diamidino-2-phenylindole) was used. The slides were examined with a reversed phase fluorescence Zeiss Axiovert microscope using filters at 488, 546 and 340/360 nm and images were acquired with an AxioCam MRC camera.

Gene expression through qRT-PCR

Total RNA was isolated from established cell lines by using TRIReagent Solution (Thermo Fisher Scientific, MA, USA). Prior PCR amplification total RNA was quantified using ND-1000 and the quality verified through Agilent 2100 Bioanalyzer (Agilent, Santa Clara, USA). DNase treatment was performed prior to cDNA synthesis by using TURBO DNA-free Kit (Invitrogen, CA, USA) according to the manufactures protocol. Reverse transcription was performed from one microgram of total RNA and the PCR amplification was run according to SuperScript III Reverse Transcriptase (Invitrogen) protocol for a final reaction volume of 20 μL. qRT-PCR was carried out in 5 μL reaction according to SYBR Select Master Mix (Applied Biosystems, MA, USA) protocol. The evaluation was performed in biological and technical duplicates using Viia 7 PCR Instrument, according to the following cycling conditions: 50°C for 2 min, 95°C for 2 min followed by 40 cycles at 95°C for 15 s and 60°C for 60 s. For each gene evaluated PCR primers were designed (primer sequence is shown in Table 1). 2-ΔΔCt was used to calculate relative gene expression and statistical comparisons were performed using GraphPad Prism (GraphPad Software Inc., La Jolla, CA). The geometrical mean of two housekeeping genes GAPDH and HPRT were used to calculate relative fold change as their expression did not vary significantly between cell lines.

NP administration and cell internalization

GNP and Chit-GNPs were administered at increasing dose concentrations ranging from 0.1 to 20 μg/mL.

Table 1. Primer sets used for qRT-PCR evaluation

Gene symbol		*Primer sequence*
BMI 1	Left	CCATTGAATTCTTTGACCAGAA
	Right	CTGCTGGGCATCGTAAGTATC
MSI 1	Left	GAGTGAGGACATCGTGGAGAA
	Right	ACATCACCTCCTTTGGCTGA
Glut-3	Left	GCCCTGAAAGTCCCAGATTT
	Right	TTCATCTCCTGGATGTCTTGG
HPRT1	Left	TGACCTTGATTTATTTTGCATACC
	Right	CGAGCAAGACGTTCAGTCCT
GAPDH	Left	CCCCGGTTTCTATAAATTGAGC
	Right	CACCTTCCCCATGGTGTCT

NP internalization within cells was analyzed through dark field microscopy and transmission electron microscopy (TEM).

For dark field microscopy assays, cells were grown in Ibidi 30 μ-Dish (50 mm) and incubated with GNP and Chit-GNP at the same nanoparticles concentrations for different periods of time (4 and 24 hrs). Dark field visualization of cells was performed on an inverted Zeiss Axio Observer Z1 microscope. Illumination of the sample was achieved using a halogen lamp (HAL100, 100 W, Zeiss) focused on the sample at a constant intensity through a high numerical immersion dark field condenser (NA=1.4), and the scattered light was collected by a LD Plan-Neofluar ×20 objective (NA=0.4, Zeiss). Images were acquired using an AxioCam Icc digital camera and processed by the ZEN software.

TEM, GM1 and OBL cell lines were incubated for 4 and 24hrs with NPs and subsequently double-fixed with 2.7% glutaraldehyde (Electron Microscopy Sciences, Hatfield, USA) for 2 hrs, and 1.5% OsO4 for 1.5 hrs (Sigma-Aldrich, St. Louis, USA). The cells were then dehydrated in acetone and embedded in EMBed-812 (Electron Microscopy Sciences, Hatfield, USA) series. Sections of 60–80 nm cut with a DiATOME diamond knife (DiATOME, USA) on a Bromma 8800 ULTRATOME III (LKB, Stockholm,Sweden) were collected on 300 mesh copper grids (Agar Scientific Ltd., Stansted, UK) and contrasted only with saturated alcoholic uranyl acetate (Merck, Darmstadt, Germany) for 7 min. Examination of the sections was performed with a JEOL JEM 1010 TEM (JEOL Ltd., Japan) operating at 80 kV acceleration voltage, and relevant images were captured using a Mega VIEW III camera (Olympus, Soft Imaging System, Germany).

Cell lines irradiation

Cell lines were irradiated with fractionated radiotherapy (3 consecutive fractions of 1 and 2 Gy) and one single fraction of 6 Gy at megavoltage energies (1.25 MV) using a Cobalt Theratron100^{R} (Best Theratronics, Ottawa, Canada) and low energy (0.3 MV) with Iridium 192 high dose rate brachytherapy source delivered by a Microselectron^{R} Elekta unit (Electa, Stockholm, Sweden).

Control experiments were performed following exactly the same irradiation protocol with GNPs and without GNPs, but without irradiation.

Cell viability after GNP administration and irradiation

After reaching 60-80% subconfluence, cells were treated with increasing concentrations of GNPs and Chit-GNPs. 24 hrs after treatment, a MTT viability test and Trypan blue-based counting were performed to assess cell viability. After removing the medium and washing three times with PBS, the yellow MTT solution [3-(4,5-dimethylthiazolyl-2)-2,5-diphenyltetrazolium bromide] was added and the plate was left at 37°C for 1 hr to allow MTT to be metabolized. Finally, the resulting purple formazan (MTT metabolite product) was resuspended in 150 μl DMSO and placed on a shaking table to mix the formazan with the solvent. The reduction of MTT to formazan takes place only when mitochondrial enzymes are active; therefore, the conversion rate can directly estimate the number of living cells. The concentration was determined by optical density at 492 nm by using a fluorescence microplate reader (Synergy 2, BioTek, Winooski, VT, USA). MTT results were also confirmed through Trypan blue staining with an automatic cell counter (EVE, NanoEnTek USA Inc.).

Statistics

All experiments were repeated at least twice and expressed as mean ± standard error of the mean (SEM) of three independent biological replicates. Statistical analyses were performed using Prism version 5.0 (GraphPad San Diego CA, USA). Statistical significance between groups was assessed by one-way ANOVA followed by Bonfferoni's multiple comparison post-test and expressed as (*) when $p<0.05$, (**) when $p < 0.01$ and (***) when $p<0.001$.

Results

Chit-GNPs are spherical NPs, with a positive zeta potential and a median size of nearly 26 nm

Colloidal gold nanoparticles displayed visible colors due to the collective oscillation of the conduction electrons in resonance with the illuminating light field. The resonant frequency of these oscillations corresponded to the so-called localized surface plasmon resonances (LSPR) which were manifested as strong UV–vis-NIR extinction bands. The successful synthesis of Chit-GNPs and GNPs

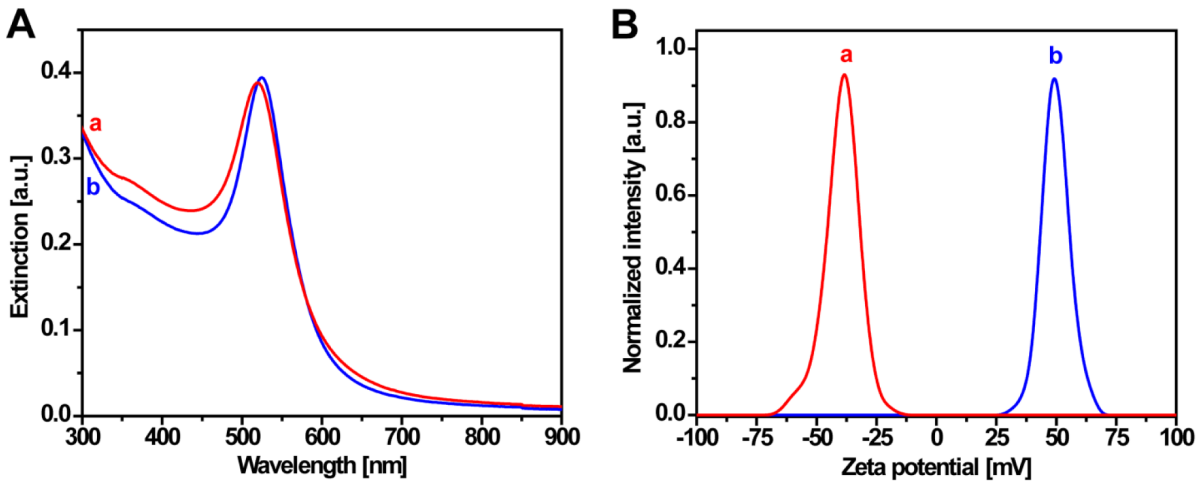

Figure 1. UV-Vis extinction spectra **(A)** and zeta-potential **(B)** of GNP (a) and Chit-GNP (b) show the dipolar plasmon resonance of spherical nanoparticles.

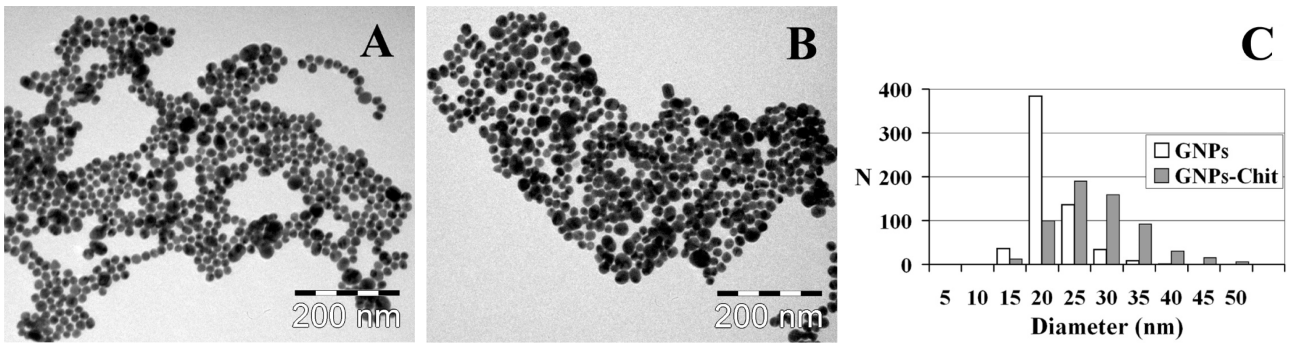

Figure 2. Transmission electron microscopy images of uncovered GNPs **(A)** and Chit-GNPs **(B)**. The size distribution for the diameters of both types of granules is represented in histogram **(C)**. N=number of particles.

was first revealed by the visual changes in solution over time. The optical spectra of colloidal solutions in Figure 1 A exhibited a dominant extinction band located at 525 nm for Chit-GNPs and at 520 nm for GNP, which represented the typical signature of the dipolar plasmon resonance of spherical NPs. Indeed, TEM analysis in Figure 2 revealed the formation of more or less dispersed GNPs (Figure 2A) and Chit-GNPs (Figure 2B) displaying prevalently spherical shapes and with diameters of 19±4 nm for GNPs and of 26±6 nm for GNPs-Chit (Figure 2C).

The zeta potential of NPs in Figure 1B differed according to their surface chemistry. Uncoated GNP had a negative surface charge (- 34 mV) due to the presence of citrate molecules at their surface, that were used as a reducing agent during the synthesis process. Chit-GNPs had a positive charge (+ 49).

Patient-derived glioblastoma cells expressed markers of GSCs and had an intrinsic resistance to radiotherapy

Apart from GM1, which was already characterized by our team in a previous paper and proved the expression of GSC markers [14], Gbl 8 and Gbl 12 also expressed markers associated with pluripotency and stemness, such as CD133, Nestin, Sox 2, Nanog, and markers expressed by neural cells, such as GFAP and NF (Figure 3).

Despite a similar expression of markers for Gbl 8 and Gbl 12, their behavior differed in terms of proliferation rate and response to treatments. The molecular characterization through RT-PCR revealed a low expression of the BMI 1 gene for both Gbl 8 and Gbl 12, whereas different expressions of MSI 1 and Glut-3 could be observed (Figure 4). These gene are also stem cell-related genes that were found to be expressed in infiltrative glioblastoma cells [15].

All patient-derived GSCs proved resistant to radiotherapy

GM1, Gbl 8 and Gbl 12 proved an intrinsic resistance to radiotherapy, despite increasing doses of irradiation (1, 2 or 6 Gy), the use of 3 consecutive fractions (of 1 and 2 Gy) or high vs low voltage

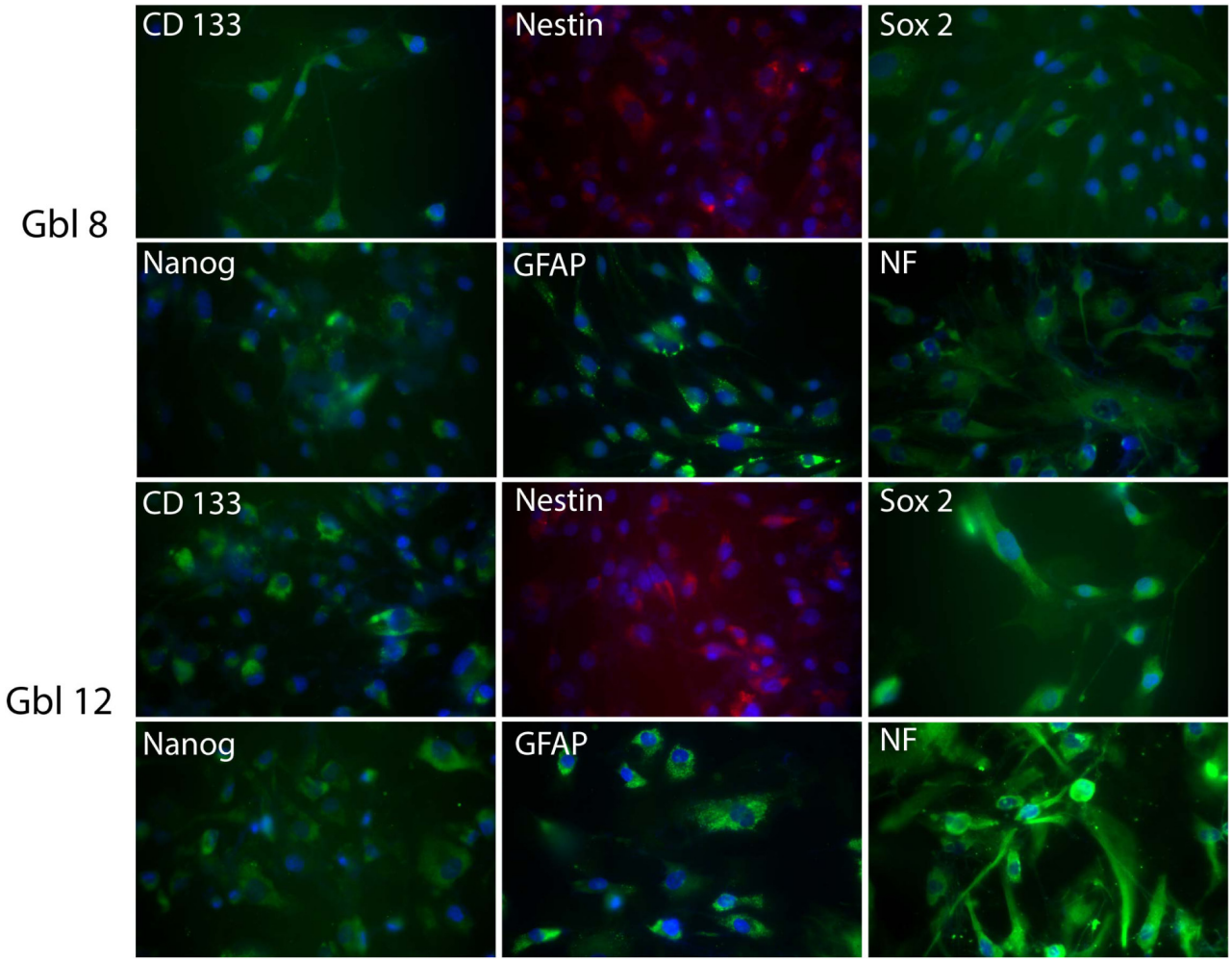

Figure 3. Immunocytochemical characterization of Gbl 8 and Gbl 12. Both cell lines express cancer stem cell markers (CD133, Nestin, Sox2, Nanog) and neural specific markers (GFAP, NF) (fluorescence microscopy ×20).

source of energy (Cobalt-60 vs Iridium 192). No change in terms of cell viability was detected in any of the irradiation protocols used (Figure 5).

Chit-GNPs were highly internalized within all GSC lines used, as opposed to uncoated GNPs. Both Chit-GNPs and GNPs internalized within the normal osteoblast cell line

Cellular uptake and intracellular trafficking of NPs analyzed by TEM

GM1 cell line. TEM examination of GM1 cells after incubation with GNPs did not reveal the presence of GNPs within the cells either after 24-h incubation (Figure 6 A,B), or after a 4-h incubation (Figure 6 C,D).

In contrast, the incubation of GM1 with Chit-GNPs resulted in an extensive internalization of Chit-GNPs (Figure 7). Many pinocytosis vesicles containing large number of Chit-GNPs (Figure 7 A,B) were found in almost all the cells. Disruption of the endosomal membrane was also found here, resulting in releasing of many other GNPs into the cytosol (Figure 7 B). This process, repeated many times, led to accumulation of huge numbers of Chit-GNPs in the cytosol, still grouped in clusters, that occupied important areas in some of the studied cells, including the proximity of nucleus

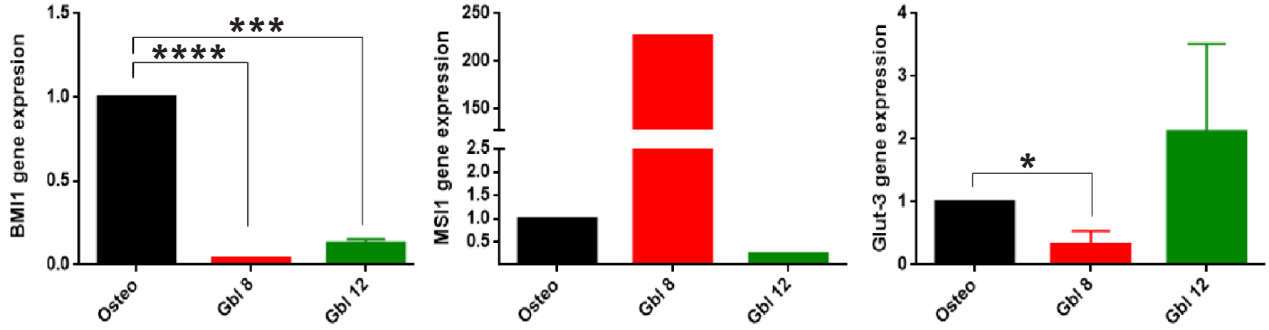

Figure 4. RT-PCR assessing gene expression of BMI 1, MSI 1 and Glut-3 in Gbl 8, Gbl 12 and osteoblasts. $p<0.05$ (*), $p<0.001$ (***) and $p<0.0001$ (****).

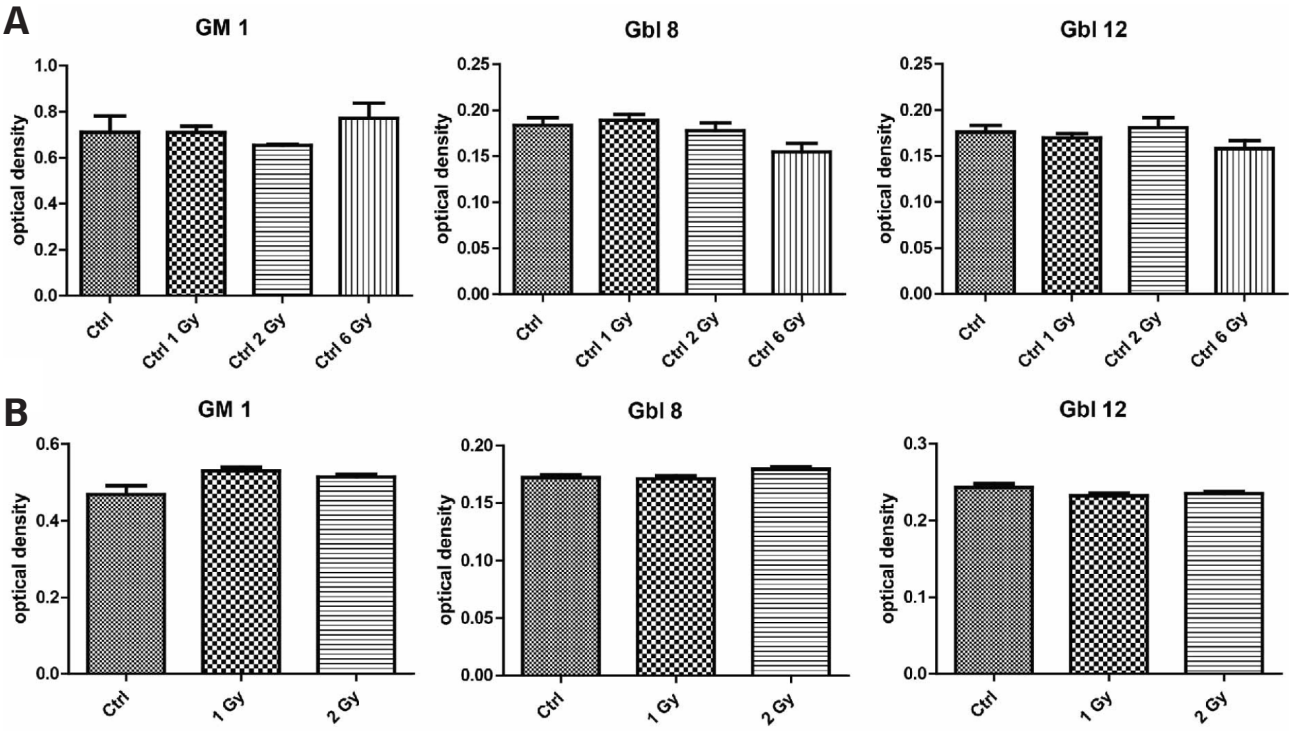

Figure 5. Cell viability as measured by MTT 48 hrs after irradiation with **(A)** Cobalt Theratron100– 3 fractions of 1 and 2 Gy in three consecutive days and one single fraction of 6 Gy were delivered. No significant difference in cell viability was detected ($p>0.05$). **(B)** Iridium 192 – No significant differences in cell viability was documented after irradiation with 1 and 2 Gy ($p>0.05$). Control arms were mock irradiated.

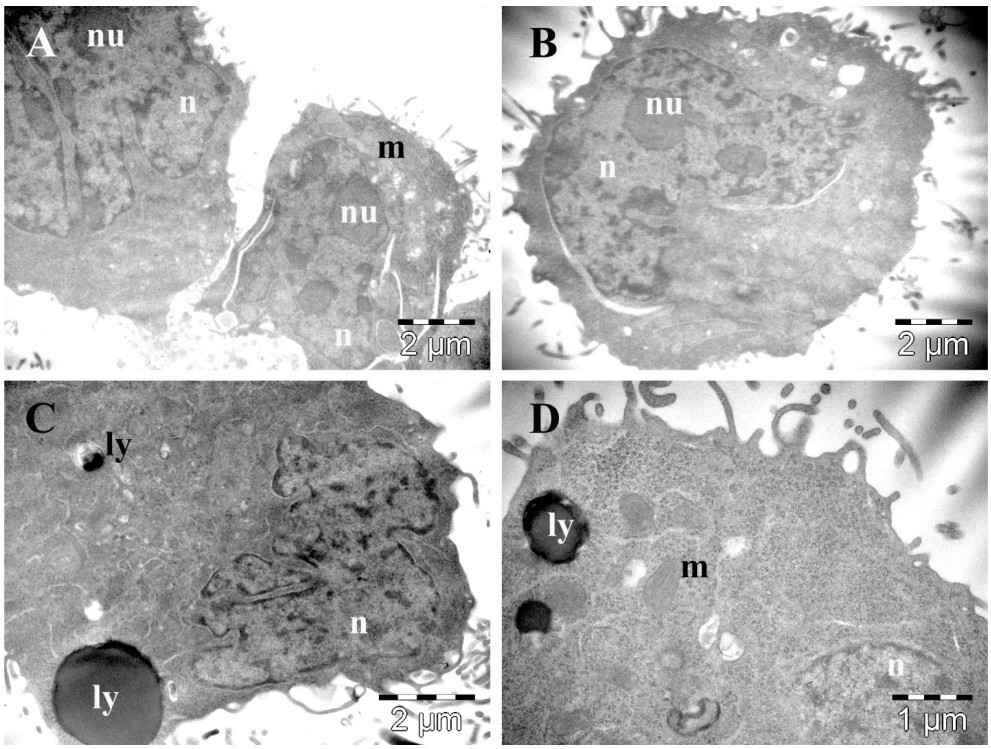

Figure 6. Transmission electron microscopy images of GM1 cells incubated with GNPs for 24 hrs **(A,B)** and for 4 hrs **(C,D)**. No GNPs were found inside the cells after either incubation time. ly:lysosomes, m:mitochondria with normal structure, n:nucleus, nu:nucleolus. Magnification **(A)** ×12.000; **(B)** ×12.000; **(C)** ×15.000; **(D)** ×25.000.

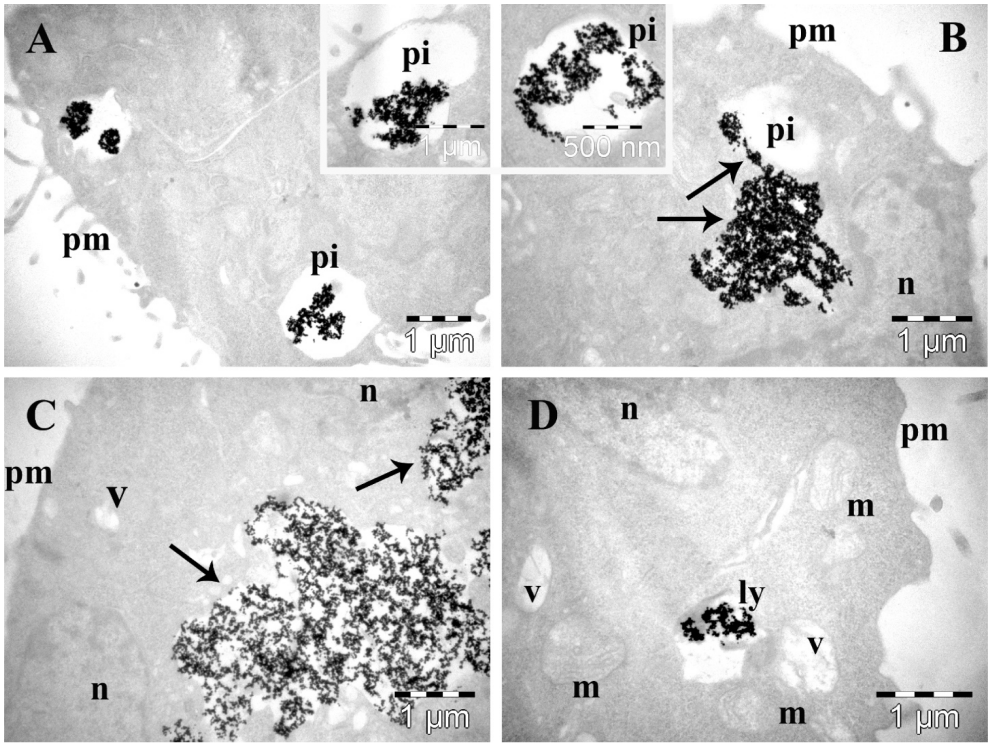

Figure 7. Transmission electron microscopy images of GM1 cells incubated with Chit-GNPs for 24 hrs. Large pinocytosis vesicles (pi) present in the proximity of plasma membrane (pm) contained numerous Chit-GNPs **(A,B)**. The Chit-GNPs were released from pinocytosis vesicles (pi) into the cytosol **(B)** and localized in some cases next to nucleus (n); arrows indicate the Chit-GNPs grouped in clusters into the cytosol. In many cells, the Chit-GNPs occupied large areas within the cytoplasm **(C)**. Rare cells contained a few lysosomes charged with clusters of Chit-GNPs **(D)**, as well as a few vacuoles (v). Chit-GNPs: Chitosan-coated gold nanoparticles, GNP: Gold nanoparticles, m:mitochondria with normal structure, n: nucleus, pi: pinocytosis vesicles, pm: plasma membrane. Magnification **(A)** ×20.000; **(B)** ×25.000; **(C)** ×25.000; **(D)** ×30.000.

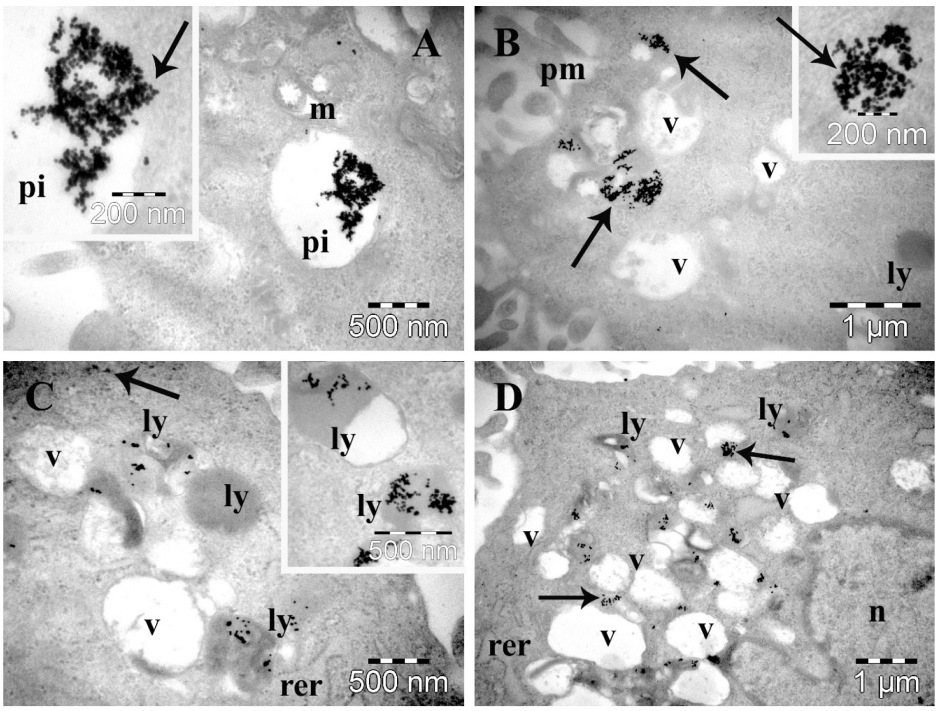

Figure 8. Transmission electron microscopy images of OBL cells incubated with GNPs for 4 hrs. Many cells contained the GNPs in pinocytosis vesicles and were observed in the proximity of plasma membrane **(A,B)**. The membrane of endosomes had the tendency to break apart on limited regions and to release the GNPs in direct contact with the cytosol **(B-D)**. Low number of GNPs was also found in lysosomes still aggregated in clusters **(C,D)**. Arrows indicate GNPs in cytosol. Chit-GNP: chitosan-coated gold nanoparticles, GNP: gold nanoparticles, ly: lysosomes, m:mitochondria, n:nucleus, pi: pinocytosis vesicles, pm: plasma membrane, rer: rough endoplasmic reticulum, v:vacuoles. Magnification **(A)** ×40.000; **(B)** ×30.000; **(C)** ×40.000; **(D)** ×20.000.

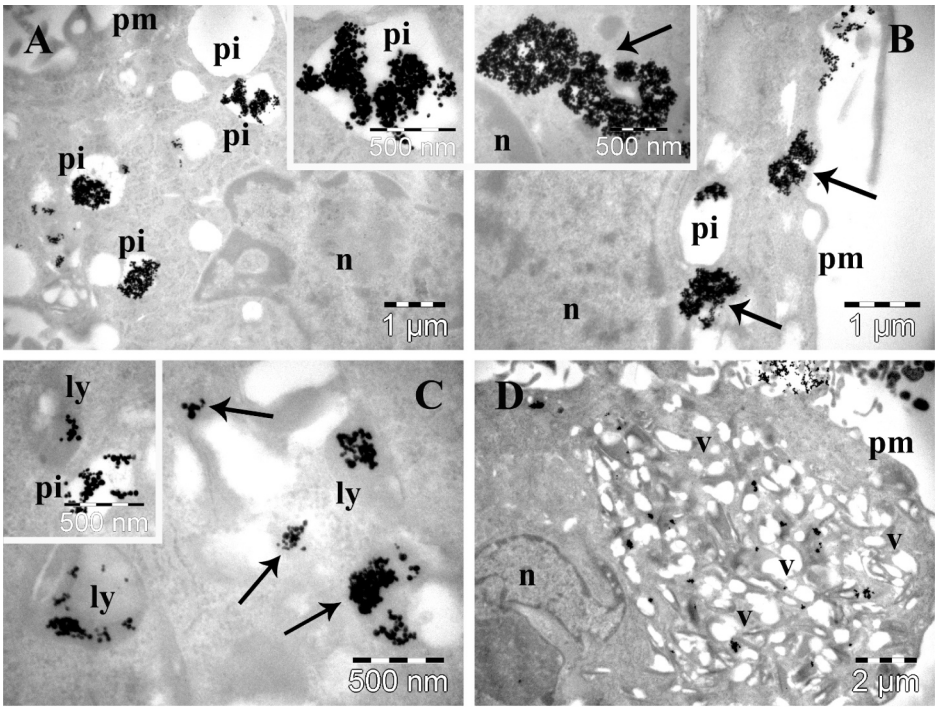

Figure 9. Transmission electron microscopy images of OBL cells incubated with Chit-GNPs for 24 hrs. A high number of pinocytosis vesicles containing Chit-GNPs, were located in the proximity of plasma membrane **(A)**. Large clusters of Chit-GNPs were dispersed in cytosol **(A-D)**, sometimes even in the proximity of nucleus, while other Chit-GNPs were still attached to plasma membrane outside the cell **(B,D)**. Arrows indicate Chit-GNPs in cytosol. Many Chit-GNPs accumulated in lysosomes **(C)**. Some cells showed extensive vacuolation of their cytoplasm **(D)**, containing a high number of vacuoles. Chit-GNP: chitosan-coated gold nanoparticles, GNP: gold nanoparticles, ly: lysosomes, n: nucleus; pi: pinocytosis vesicles, pm: plasma membrane, v:vacuoles. Magnification **(A)** ×20.000; **(B)** ×25.000; **(C)** ×60.000; **(D)** ×10.000.

(Figure 7 B,C). Also, Figure 7 D shows an important accumulation of Chit-GNPs within the lysosomes. The Chit-GNPs-containing lysosomes showed a tendency for vacuolation (Figure 7 D), although this aspect could also indicate a recent fusion of pinocytosis vesicles with lysosomes.

Osteoblast (OBL) cell line. TEM examination of OBL cultured cells after 24-h incubation revealed the presence of GNPs in their cytoplasm (Figure 8), while no GNPs were found inside the nucleus. A relatively high number of GNPs were located in pinocytosis vesicles in the proximity of plasma membrane (Figure 8 A), indicating that GNPs were introduced in cells by endocytosis. In many such endosomes, GNPs showed a tendency to get out into the cytosol by disrupting their membranes (Figure 8A). As a direct consequence, large clusters of GNPs were present in the cytoplasm, in direct contact with the cytosol, and being more or less aggregated (Figure 8 B). In some OBL cells, GNPs were also found in lysosomes – most of them containing a low number of GNPs, usually aggregated in small clusters (Figure 8 C). As a particular ultrastructural aspect, some cells displayed a high degree of vacuolation (Figure 8 D). In such cells, GNPs were also observed both as clusters between the vacuoles, and inside the lysosomes.

Similar to GM1, TEM examination of OBL after 24-h incubation with Chit-GNPs revealed the presence of Chit-GNPs in the cytoplasm (Figure 9). Compared to their counterparts incubated with uncoated GNPs, Chit-GNP treated OBL presented a higher number of NP-containing pinocytosis vesicles, with a higher NP concentration within the vesicles and more and larger Chit-GNP clusters in the cytosol (Figure 9 A-D). Also, the number of Chit-GNPs concentrated into the lysosomes was higher than in the previous experimental group (Figure 9 C). A low number of cells were highly vacuolated with vacuoles that occupied almost the entire cytoplasm and clusters of GNPs were observed between them (Figure 9 D).

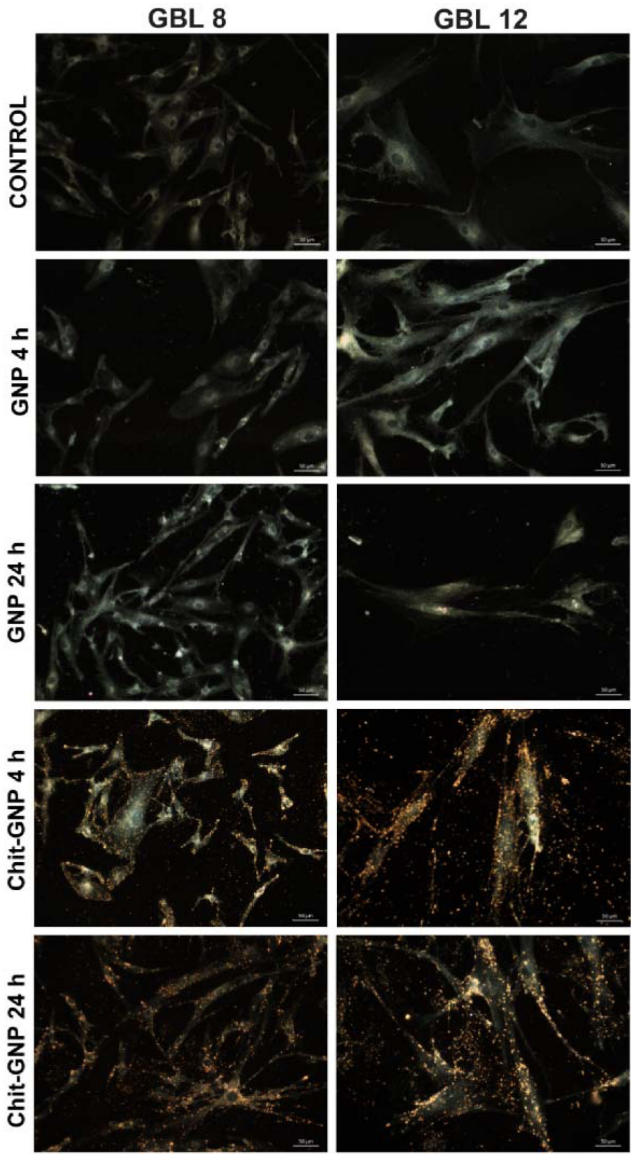

Figure 10. Dark field microscopy images of control cells, cells incubated with GNP and Chit-GNP for 4 and 24 hrs. An increased cell internalization of Chit-GNP may be observed, whereas no GNP cellular uptake could be evidenced.

Cellular uptake of GNPs analyzed by dark-field imaging

The high scattering cross sections of gold nanoparticles together with their small sizes and favorable surface chemistries make them ideal choices for cellular-based imaging applications. Dark-field microscopy represents one of the most popular bioimaging methods based on gold nanoparticles. GNPs are known to strongly scatter visible light due to their surface plasmon resonances, therefore they can be easily visualized using dark-field microscopy.

Cells were incubated at the same concentration of GNP and Chit-GNP for 4 and 24 hrs. Similar to TEM results, uncoated GNP were not internalized in neither of the GSCs investigated in this study, whereas Chit-GNP presented a robust uptake in all tumor cell lines and osteoblasts. The strong scattering originating from Chit-GNP can be observed as orange-red spots localized mostly throughout all the cytoplasm within internal vesicles such as endosomes and lysosomes (Figure 10). Also, a large number of NPs was also found to be in the vicinity of cellular membranes.

NPs displayed a different internalization and cell distribution at 4 compared to 24 hrs of incubation. While 4-h incubation revealed the presence of individual or slightly agglomerated NPs

in the form of orange-redish bright spots, the 24-h incubation resulted in a superior aggregation of NPs inside cellular organelles, attributable to the very high concentration of NPs internalized per cell. This aggregation can be identified as larger, nearly white spots inside cells and even bound at the cell membrane. It is worth mentioning that no NP internalization into the nuclei was observed for neither cell line which is plausible as the size of GNP does not permit to cross the nuclear membrane via the nuclear pores, and neither specific nucleus targeting agent was used.

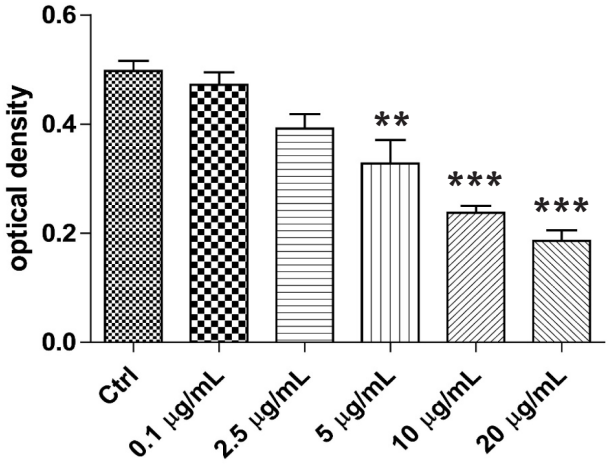

Figure 11. MTT viability assay of GM1 after 24-h incubation with several concentrations of Chit-GNP. Increasing doses of Chit-GNP were used (0.1 µg/mL, 2.5 µg/mL, 5 µg/mL, 10 µg/mL and 20 µg/mL) and cell viability was affected in a dose-dependent manner. Compared to control, p<0.01 (**) and p <0.001 (***).

Chit-GNPs displayed an important anti-tumor effect even at small concentrations

To determine cell viability, cells were assessed for mitochondrial activity using the MTT assay. Cells were exposed to GNPs and Chit-GNPs at increasing concentrations of 0.1 µg/mL, 2.5 µg/mL, 5 µg/mL, 10 µg/mL and 20 µg/mL, for 4 and 24 hrs. Viability was unaffected by GNPs, while a dose-dependent cytotoxicity was observed with Chit-GNPs (Figure 11). Both 10 µg/mL and 20 µg/mL concentrations significantly reduced cell viability, however, we chose to work with 10 µg/mL because the higher 20 µg/mL concentration produced a large number of Chit-GNP aggregates, that were visible even in light microscopy. A significant reduction of cell viability was observed at 8-10 µg/mL

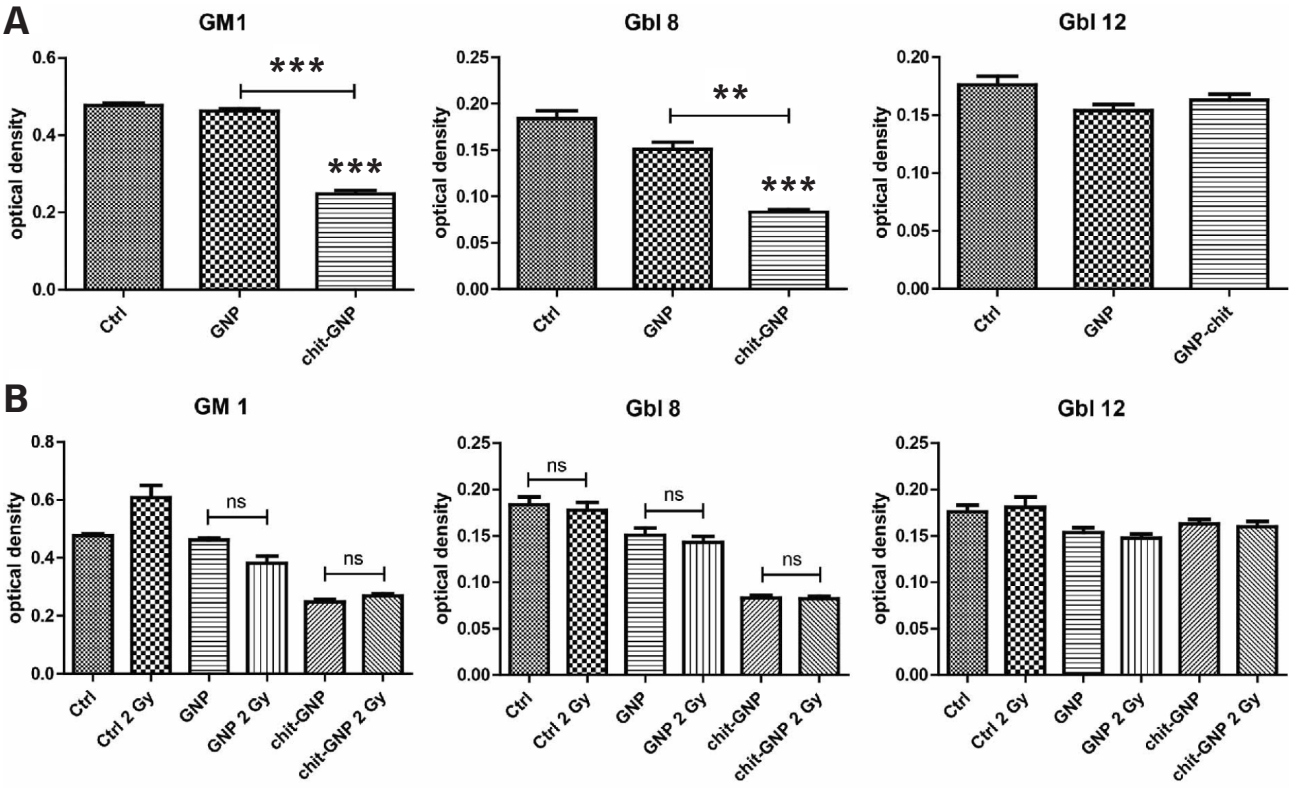

Figure 12. MTT viability assay performed 24 hrs after treatments. **(A)** GSCs were treated with 10 µg/mL of GNP and Chit-GNP. GM1 and Gbl 8 cell lines were significantly affected by treatment with Chit-GNP, by reducing to half their cellular viability compared to control, p ≤0.001 (***) and compared to uncoated GNP, p ≤0.001 (***) for GM1 and p ≤0.01 (**) for GBL8. Gbl 12 was not affected by the tested NPs (p >0.05). **(B)** Comparison between untreated, treated with GNP and Chit-GNP and their irradiated counterparts showed no difference in terms of cell viability when 2 Gy irradiation was applied. ns: non significant (p >0.05).

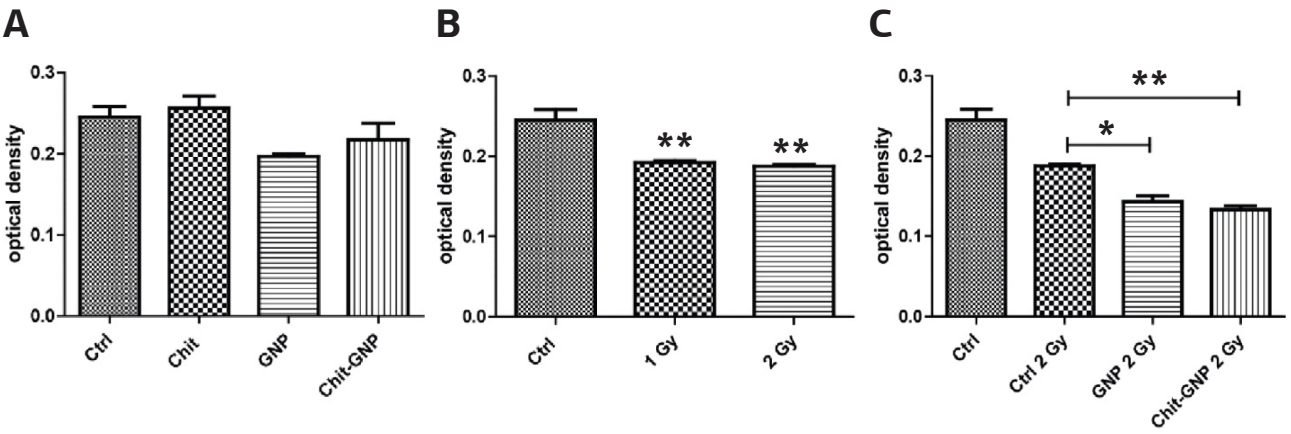

Figure 13. Effect on normal cell line - osteoblasts (OBL) - MTT viability assay performed 24 hrs after treatments. **(A)** GNP and Chit-GNP did not reduce significantly the cell viability of OBL compared to control ($p > 0.05$). **(B)** Irradiation – OBL viability was significantly reduced after irradiation at 1 and 2 Gy (**$p < 0.01$). **(C)** When both irradiation and NPs were administered, GNP and Chit-GNP enhanced significantly the cytotoxic effect of irradiation: irradiated control vs irradiated GNP (*$p < 0.05$) and irradiated control vs irradiated Chit-GNP (**$p < 0.01$).

concentration of Chit-GNP for GM1 and Gbl 8 both compared to control and to uncoated GNPs (Figure 12 A). Solvent controls with chitosan were also assessed for their influence on cell viability, and were found to have none.

GNPs were cytotoxic by themselves and RT did not add an additional benefit

To investigate whether GNP/Chit-GNPs could sensitize cells to irradiation, GSCs were incubated 24 hrs with NPs, then irradiated with 2 Gy fractions from Cobalt Theratron100 or Iridium 192 source. Cell viability was compared between untreated, GNP, Chit-GNP and their irradiated counterparts, but failed to prove any additional benefit when irradiation was delivered (Figure 12 B).

Chit-GNPs displayed a selective cytotoxic effect on tumor cells and left normal cells unaffected. Osteoblasts were sensitized to irradiation when treated with gold NPs

Primary human osteoblasts (OBL) were impaired by irradiation, as shown by the viability assay performed 24 hrs after irradiation with 1 Gy and 2 Gy. GNP and Chit-GNP were not toxic by themselves for OBL, but when irradiation was applied 24 hrs after NP administration, both GNP and Chit-GNP sensitized cells to irradiation and significantly decreased cell viability compared to unirradiated cells or to irradiated cells without NPs (Figure 13).

Discussion

In this study, we aimed to synthetize a class of gold nanoparticles that is highly internalized within glioblastoma stem-like cells and to test if such a compound would sensitize radio-resistant cells to irradiation.

Chitosan, a polysaccharide derivative of chitin, was used to coat gold nanoparticles due to its biocompatibility, safe toxicity profile, its ability to interact and permeate cell membranes and also its ability to release the content in acidic conditions [16,17]. Moreover, chitosan was reported to have a role even in tumor targeting due to its similar structure with hyaluronic acid, a natural ligand for CD44, which is a receptor mainly expressed by cancer stem cells [18]. Chitosan was already reported as a useful reducing agent for rapid synthesis of GNPs and subsequently used for drug delivery applications [19].

Our work generated chitosan-capped gold nanoparticles of spherical shape, with a mean diameter of 26 nm and a positive charge of + 49 mV. These physico-chemical characteristics enabled Chit-GNPs to be highly internalized within GSCs and osteoblasts via pinocytosis and to form numerous and large aggregates of NPs within the cytoplasm, lysosomes and near the nucleus. Their accumulation within the lysosomes might be a major advantage for further drug delivery applications because chitosan has the ability of releasing the content in acidic conditions. Surprisingly, no uncoated GNPs have been observed at 4 and 24 hrs in any of the analyzed GSCs. This huge difference in cellular uptake may be explained by the positive charge of Chit-GNP that are easily attracted by the negatively-charged cells, whereas the negative charge of naked GNP might impede cell internalization due to repulsion forces between cells and NPs [8]. Another explanation might be that in the lack of additional stabilizing agents, citrate capped

GNPs present only electrostatic stability which did not protect NPs from the undesired aggregation in biological medium. As a consequence, larger NP assemblies created upon incubation may be hardly internalized by cells.

However, the normal cell line used had a completely different behavior when incubated with uncoated GNPs because GNPs were found in a large number within the cytoplasm, in different locations (pinosomes, cytosol, lysosomes). Chit-GNPs were internalized following a common pattern in both GSCs and osteoblasts, with a higher accumulation of Chit-GNPs in GM1 cells compared to osteoblasts [18].

Another aim of our study was to test whether Chit-GNPs or GNPs could sensitize highly radioresistant GSCs to radiotherapy. We chose gold for NP development not only for their inert properties, but especially because heavy metals are hypothesized to locally enhance the response to irradiation when an external source of photon irradiation is applied. The physical basis is by the photoelectric effect, which is significant at low energies (≤0.3 MV) and also dependent on the atomic mass (Z) of the target (and therefore more pronounced for the gold). At higher energies, the Compton effect (independent of the Z) exceeds the photoelectric effect and the enhancement ratio decreases. This phenomenon has been described in several studies as an efficient anticancer strategy [20-23]. Joh et al. proved that gold NPs significantly increased cellular DNA damage inflicted by ionizing radiation in human U251 GBM-derived cell lines and resulted in reduced clonogenic survival (with dose-enhancement ratio of ~1.3). Importantly, the combination of gold NPs and irradiation increased survival of mice with orthotopic GBM tumors [24].

Despite having a huge Chit-GNP cellular uptake, our data did not confirm the results of Joh et al., as our study did not show a radiosensitization of GSCs when Chit-GNP/GNP were administered in combination with irradiation. However, the radio-enhancer effect of NPs was observed on normal cells, which were slightly sensitive to irradiation and further sensitized when both GNPs and Chit-GNPs were used. This suggests that GNP/Chit-GNPs might be able to enhance the response to radiotherapy only if the cell line is partly sensitive to irradiation as an intrinsic feature. Joh et al. used the U251 glioblastoma cell line that partly responded to irradiation even without GNPs, whereas our GSCs were highly resistant to any of the irradiation doses/ protocols used.

It has been suggested that gold NP size might also influence their impact on radiotherapy response. Recent data show that 50 nm particles had the highest enhancement factor when irradiated with 6 MVp photons compared to NPs of 14 and 74 nm, but this was explained by the fact that 50 nm NPs had the highest cellular uptake [21]. Our 26 nm-sized Chit-GNPs proved to have a suitable size for cell internalization and persistence within cells for at least 24 hrs. Such dimension should also ensure a proper migration within the stiff tumor interstitium of glioblastoma [8].

A surprising result of our study was that small μg/mL concentrations of Chit-GNPs proved highly cytotoxic for two of the GSCs used and their cytotoxicity was selective for the tumor lines and did not affect the normal cell line. This could be explained by the increased intracellular accumulation of both chitosan and gold, however, each component used as monotherapy is harmless for GSCs.

The selective cytotoxicity of Chit-GNPs for GSCs could be due to the major NP internalization within GSCs, which is larger compared to normal osteoblasts. However, numerous NP aggregates have also been observed within normal cells, that makes this assumption less probable. The study of Rao et al. generates a hypothesis because the authors observed that although their chitosan-decorated product, nDOX could bind to the CD44 receptors on the cancerous mammosphere cells including cancer stem-like cells, it does not necessarily bind to the CD44 receptors highly expressed on non-cancerous stem cells. They showed that no apparent binding could be observed between nDOX and the CD44 receptors overexpressed on the normal primary human adipose-derived stem cells either cultured in 3D spheres or under 2D adherent culture which suggests that CD44 could have different isoforms expressed on cancer stem-like cells compared to normal stem cells [18].

Considering that two of our three GSCs responded to Chit-GNP, we tried to identify several differences between the three cell lines, that could explain their different response. Their molecular and immunocytochemical characterization exhibit nearly the same features regarding their stemness. However, a slightly different molecular profile appears to exist between Gbl 12 and Gbl 8, with a higher MSI 1 expression for Gbl 8 and a higher Glut 3 expression for Gbl 12. High expression level of MSI 1 positively correlates with advanced grade of glioblastoma, where MSI1 increases the growth of glioblastoma [25]. This feature would be in line with the high proliferative capacity of Gbl 8. The slightly higher Glut 3 expression of Gbl 12 might suggest that Gbl 12 extracts nutrients with higher affinity and possibly has a more harmful behavior considering the association between Glut 3 and poor survival in brain tumors and other cancers

[26]. Although it is possible that metabolic differences between cells might be responsible for different response to treatment, further research is necessary to make valid assumptions.

The low doses of NPs and the small radiation doses utilized in this study compared to other studies were specifically chosen due to safety reasons from a translational point of view. High doses of NPs would result in an increased accumulation of excipients within the brain and higher fractions of irradiation would be too toxic for the normal brain tissue. Nevertheless, after not observing a radio-enhancement effect at 1 and 2 Gy doses, we checked also a dose-level of 6 Gy/fr, trying to overcome the intrinsic radioresistance of our cell lines but, again, without significant difference. One limitation of our study could be the use of MTT test for assessing the response to irradiation. However, we did confirm the lack of response to irradiation through automatic cell counting and clonogenic assays (data not shown – negative results.

Conclusions

Chitosan-capped gold nanoparticles are produced in an easy, reproducible and cost-effective way. In this study, we have proved that Chit-GNPs have a selective cytotoxic effect on patient-derived glioblastoma stem cells even when used in small concentrations and that this effect occurs irrespective of cell irradiation. The Chit-GNPs have a huge cellular uptake and they accumulate within the cytosol via pinocytosis, in the lysosomes and near the nucleus. On the contrary, uncoated GNP were not observed within any of the GSC lines analyzed.

Radiotherapy failed to add an additional benefit when administered to these highly resistant GSC lines and Chit-GNP did not sensitize GSC to irradiation. However, our results on osteoblasts suggest that GNP and Chit-GNP may further sensitize cell to irradiation, if such cells have an intrinsic radiosensitivity.

The highly increased NP accumulation within cancer stem cells and especially their selective cytotoxic effect on tumor cells, make Chit-GNP an attractive component of the armamentarium against glioblastoma and a promising backbone for anticancer drug delivery.

Acknowledgements

This research was financially supported by an EUFISCDI National Grant - PNII-RU-TE-2014-4-0225 (ENERGY), Competition for Young Teams, Program for Human Resources. M.A. was also financed by a research grant for PhD Fellows (contract number 7690/2/15.04.2016) offered by the University of Medicine and Pharmacy (Cluj-Napoca).

Conflict of interests

The authors declare no conflict of interests.

References

1. Stupp R, Hegi ME, Mason WP et al. Effects of radiotherapy with concomitant and adjuvant temozolomide versus radiotherapy alone on survival in glioblastoma in a randomised phase III study: 5-year analysis of the EORTC-NCIC trial. Lancet Oncol 2009;10:459-66.
2. Chen J, Li Y, Yu TS et al. A restricted cell population propagates glioblastoma growth after chemotherapy. Nature 2012;488:522-6.
3. Auffinger B, Tobias AL, Han Y et al. Conversion of differentiated cancer cells into cancer stem-like cells in a glioblastoma model after primary chemotherapy. Cell Death Differ 2014;21:1119-31.
4. Bao S, Wu Q, McLendon RE et al. Glioma stem cells promote radioresistance by preferential activation of the DNA damage response. Nature 2006;444:756-60.
5. Lathia JD, Mack SC, Mulkearns-Hubert EE et al. Cancer stem cells in glioblastoma. Genes Dev 2015;29:1203-17.
6. Aldea MD, Petrushev B, Soritau O et al. Metformin plus sorafenib highly impacts temozolomide resistant glioblastoma stem-like cells. JBUON 2014;19:502-11.
7. Dean M, Fojo T, Bates S. Tumour stem cells and drug resistance. Nat Rev Cancer 2005;5:275-84.
8. Aldea M, Florian IA, Kacso G et al. Nanoparticles for Targeting Intratumoral Hypoxia: Exploiting a Potential Weakness of Glioblastoma. Pharm Res 2016;33:2059-77.
9. Aldea M, Craciun L, Tomuleasa C et al. Repositioning metformin in cancer: genetics, drug targets, and new ways of delivery. Tumour Biol 2014;35:5101-10.
10. Jain S, Coulter JA, Butterworth KT et al. Gold nanoparticle cellular uptake, toxicity and radiosensitisation in hypoxic conditions. Radiother Oncol 2014;110:342-7.
11. McMahon SJ, Hyland WB, Muir MF et al. Biological consequences of nanoscale energy deposition near irradiated heavy atom nanoparticles. Sci Rep 2011;1:18.
12. Turkevich J CSP, Hillier J. A study of the nucleation and growth processes in the synthesis of colloidal gold. Discuss Faraday Soc 1951;11:55-75.

13. Potara M, Maniu D, Astilean S. The synthesis of biocompatible and SERS-active gold nanoparticles using chitosan. Nanotechnology 2009;20:315602.
14. Tomuleasa C, Soritau O, Rus-Ciuca D et al. Functional and molecular characterization of glioblastoma multiforme-derived cancer stem cells. J BUON 2010;15:583-91.
15. Munthe S, Petterson SA, Dahlrot RH et al. Glioma Cells in the Tumor Periphery Have a Stem Cell Phenotype. PLoS One 2016;11:e0155106.
16. Amidi M, Hennink WE. Chitosan-based formulations of drugs, imaging agents and biotherapeutics. Preface. Adv Drug Deliv Rev 2010;62:1-2.
17. Boyles MS, Kristl T, Andosch A et al. Chitosan functionalisation of gold nanoparticles encourages particle uptake and induces cytotoxicity and pro-inflammatory conditions in phagocytic cells, as well as enhancing particle interactions with serum components. J Nanobiotechnology 2015;13:84.
18. Rao W, Wang H, Han J et al. Chitosan-Decorated Doxorubicin-Encapsulated Nanoparticle Targets and Eliminates Tumor Reinitiating Cancer Stem-like Cells. ACS Nano 2015;9:5725-40.
19. Bhumkar DR, Joshi HM, Sastry M et al. Chitosan reduced gold nanoparticles as novel carriers for transmucosal delivery of insulin. Pharm Res 2007;24:1415-26.
20. Rahman WN, Bishara N, Ackerly T et al. Enhancement of radiation effects by gold nanoparticles for superficial radiation therapy. Nanomedicine 2009;5:136-42.
21. Chithrani DB, Jelveh S, Jalali F et al. Gold nanoparticles as radiation sensitizers in cancer therapy. Radiat Res 2010;173:719-28.
22. Liu CJ, Wang CH, Chen ST et al. Enhancement of cell radiation sensitivity by pegylated gold nanoparticles. Phys Med Biol 2010;55:931-45.
23. Butterworth KT, Coulter JA, Jain S et al. Evaluation of cytotoxicity and radiation enhancement using 1.9 nm gold particles: potential application for cancer therapy. Nanotechnology 2010;21:295101.
24. Joh DY, Sun L, Stangl M et al. Selective targeting of brain tumors with gold nanoparticle-induced radiosensitization. PLoS One 2013;8:e62425.
25. Chen HY, Lin LT, Wang ML et al. Musashi-1 regulates AKT-derived IL-6 autocrinal/paracrinal malignancy and chemoresistance in glioblastoma. Oncotarget 2016;7:42485-501.
26. Flavahan WA, Wu Q, Hitomi M et al. Brain tumor initiating cells adapt to restricted nutrition through preferential glucose uptake. Nat Neurosci 2013;16:1373-82.